Published in final edited form as:
Kidney Int. 2009 February ; 75(3): 295–303. doi:10.1038/ki.2008.505.

Serine 269 phosphorylated aquaporin-2 is targeted to the apical membrane of collecting duct principal cells

Hanne B. Moeller[1], **Mark A. Knepper**[2], and **Robert A. Fenton**[1]

[1]The Water and Salt Research Center, Institute of Anatomy, University of Aarhus, Aarhus, Denmark

[2]Laboratory of Kidney and Electrolyte Metabolism, National Heart, Lung, and Blood Institute, National Institutes of Health, Bethesda, Maryland, USA

Abstract

Trafficking of the water channel aquaporin-2 to the apical plasma membrane of the collecting duct is mediated by arginine vasopressin, rendering the cell permeable to water. We recently identified a novel form of aquaporin-2 that is phosphorylated at serine-269 (pS269-AQP2). Using antibodies specific for this form of the water channel, we detected rat and mouse pS269-AQP2 in the connecting tubule and throughout the collecting duct system. Using confocal immunofluorescence microscopy with organelle-specific markers and immunogold electron microscopy, we found that pS269-AQP2 was found only on the apical plasma membrane of principal cells. In vasopressin-deficient Brattleboro rats, pS269-AQP2 was undetectable but dramatically increased in abundance after these rats were treated with [deamino-Cys-1, d-Arg-8]vasopressin (dDAVP). This increase occurred only at the apical plasma membrane, even after long-term dDAVP treatment. Following dDAVP there was a time-dependent redistribution of total aquaporin-2 from predominantly intracellular vesicles to the apical plasma membrane, clathrin-coated vesicles, early endosomal compartments, and lysosomes. However, pS269-AQP2 was found only on the apical plasma membrane at any time. Our results show that S269 phosphorylated aquaporin-2 is exclusively associated with the apical plasma membrane, where it escapes endocytosis to remain at the cell surface.

Keywords

phosphorylation; vasopressin; endocytosis; exocytosis; immunohistochemistry; aquaporin water channel

Renal water permeability of the mammalian collecting duct is regulated by arginine vasopressin (AVP), which is released from the posterior pituitary gland in response to increased plasma osmolality or a reduction in the effective circulating blood volume. The antidiuretic effect of AVP is mediated by the binding of AVP to the type 2 vasopressin

Correspondence: Robert A. Fenton, The Water and Salt Research Center, Institute of Anatomy (Building 1233), University of Aarhus, Aarhus DK-8000, Denmark. rofe@ana.au.dk.

DISCLOSURE

All the authors declared no competing interests.

SUPPLEMENTARY MATERIAL

Table S1. Colocalization analysis of pS269-AQP2 with organelle-specific markers.

Figure S1. Total AQP2 is associated with lysosomes.

Supplementary material is linked to the online version of the paper at http://www.nature.com/ki

receptor in the basolateral membrane of the collecting duct (CD) principal cell. Acutely, this results in the translocation of intracellular vesicles containing aquaporin-2 (AQP2) to the apical plasma membrane, rendering the cell permeable to water.[1]

A critical event in AVP-mediated translocation of AQP2 to the apical plasma membrane is phosphorylation of the C-terminal tail of AQP2 at serine 256 (S256). This is demonstrated in *in vitro* cell culture systems[2–4] and in experimental animal models.[5,6]

In addition to S256, phospho-proteomic analysis of native rat inner medullary CD (IMCD) cells determined that S256 is part of a polyphosphorylated region in the COOH terminal tail of AQP2.[7] This region contains four AVP-regulated phosphorylation sites, namely S256, S261, S264, and S269. Within the principal cell, pS261-AQP2 and pS264-AQP2 are localized at different intracellular regions[8,9] and are diversely regulated by AVP. However, recent studies failed to show a direct role for S261 phosphorylation in AQP2 trafficking.[10]

In this study, we examined the cellular and subcellular localizations and AVP-mediated regulation of AQP2 phosphorylated at S269 (pS269-AQP2). We found that pS269-AQP2 was localized exclusively in the apical plasma membrane of connecting tubule (CNT) cells, CD principal cells, and IMCD cells. In addition, chronic or acute AVP administration *in vivo* regulates the extent of S269-AQP2 phosphorylation. We propose that S269 phosphorylation is critical for the apical plasma membrane retention of AQP2 after AVP-stimulated trafficking.

RESULTS

Cellular and subcellular distribution of pS269-AQP2

Distribution of pS269-AQP2 was determined by the immunohistochemistry of the normal rat and mouse kidney sections. In both species, pS269-AQP2 labeling was observed within CD cells (Figure 1a–f). Labeling intensity was strongest in cortical and medullary CDs, with little labeling associated with IMCD. In all labeled tubules, staining was only associated with the apical plasma membrane (Figure 1, insets). No basolateral staining was observed in any region of the kidney.

A complete absence of labeling in AQP2 knockout mice as compared with control (Figure 2a and b) confirmed the specificity of the anti-pS269 antibody for AQP2. To demonstrate that for both immunohistochemistry, and that at the concentration used in our studies, the anti-pS269 antibody was specific for pS269-AQP2, we performed a number of immunostaining controls. Pre-absorption of pS269-AQP2 with a synthetic pS269-AQP2 phosphopeptide completely abolished labeling (Figure 2d). In contrast, pre-absorption with either a synthetic non-phosphorylated peptide (Figure 2c) corresponding to the same region or a pS264-AQP2 phosphopeptide (Figure 2e) did not affect pS269-AQP2 labeling. In addition, phosphatase treatment of rat kidney sections *in vitro* resulted in a reduction in pS269-AQP2 labeling (Figure 2f and g). Taken together, these results indicate that the staining of the apical plasma membrane observed in rat and mouse is specific for pS269-AQP2.

Double immunofluorescence labeling with a marker for the CNT, calbindin (Figure 3a) showed that pS269-AQP2 is detected at low levels in CNT. Double labeling with the intercalated cell marker H^+-ATPase showed that within the CD, pS269-AQP2 is restricted to principal cells (Figure 3b). Double immunofluorescence labeling with an NH_2-terminus total AQP2 antibody showed partial colocalization (R_{total} 0.37 ± 0.06) between pS269-AQP2 and total AQP2 in all CDs (Figure 3c–e). In contrast to pS269-AQP2, total AQP2 was more broadly distributed (Figure 3f) with prominent intracellular labeling and some basolateral

staining observed. In all tubules, colocalization with pS269-AQP2 (Figure 3g) was restricted to the apical plasma membrane region (Figure 3h).

Immunogold electron microscopy of normal Wistar rat kidney sections demonstrated that in CD principal cells, pS269-AQP2 was restricted to the apical plasma membrane (Figure 4a). In all cells, gold particles are observed only in association with the plasma membrane (Figure 4a, inset). After short-term [deamino-Cys-1, d-Arg-8]-vasopressin (dDAVP) treatment (30 min), we observed a marked increase in pS269-AQP2 labeling in the apical plasma membrane (Figure 4b). After dDAVP treatment for this time period, all gold particles were in direct association with the apical plasma membrane (Figure 4b, inset). Under both conditions examined, we never observed gold particles in association with the basolateral membrane (Figure 4c). These results suggest that there is a large increase in pS269-AQP2 abundance after dDAVP exposure (see later).

To further define the subcellular distribution of pS269-AQP2, double immunofluorescence labeling was performed with anti-pS269 and a variety of established subcellular markers. No colocalization was observed with the basolateral membrane marker E-cadherin, the medial Golgi marker *GS28*, the *cis*-Golgi matrix marker GM130, the *cis*-Golgi marker p115, the *trans*-Golgi network marker *Vti1a*, the early endosome marker EEA1, and the lysosomal marker Cathepsin D (Figure 5, Table S1). Although a small degree of colocalization was observed with the clathrin-coated vesicle marker Adaptin-β (Figure 5g) in some apical regions of the cell, numerous Adaptin-β-positive, but pS269-AQP2-negative compartments were observed at the apical plasma membrane. These results confirm that pS269-AQP2 resides only in the apical plasma membrane domain.

Effect of short-term vasopressin treatment on pS269-AQP2

Normal Wistar rats or AVP-deficient Brattleboro rats were treated for 30 min with the V_2-selective vasopressin analog dDAVP to determine the effects of short-term AVP treatment on pS269-AQP2 abundance. Semiquantitative immunoblotting on inner medulla protein homogenates showed that the total abundance of AQP2 was not significantly changed in response to dDAVP treatment (Figure 6). Conversely, pS269-AQP2 abundance increased significantly in response to treatment, indicating that phosphorylation of AQP2 at this site is regulated acutely by AVP *in vivo*. Surprisingly, in addition to 29 kDa non-glycosylated form of AQP2, in Wistar rats, the anti-pS269 antibody detected an additional band at approximately 32 kDa. The molecular identity of this higher-molecular-weight moiety is currently unknown. It could represent a form of AQP2 that has been chemically modified, for example by ubiquitination,[11] but the small-molecular-weight change makes this unlikely. In non-stimulated Brattleboro rats, there was a complete absence of pS269-AQP2 immunoreactivity. These results were confirmed by immunohistochemistry on kidney sections from Brattleboro rats treated with either vehicle or dDAVP for 20 min. In vehicle-treated animals, no pS269-AQP2 labeling was detected in the cortex, ISOM, or IMCD (Figure 7a–c). Strong apical labeling was observed in all CDs after dDAVP treatment (Figure 7d–f). For comparison, labeling of pS256-AQP2 was performed under similar conditions (Figure 7g–l). Strong intracellular labeling of pS256-AQP2 is observed in control conditions. After 20 min dDAVP treatment, pS256-AQP2 labeling intensity increases predominantly in the apical plasma membrane. Taken together, these results suggest that pS269-AQP2 is dependent on the presence of AVP and that AVP increases pS269-AQP2 only at the apical plasma membrane.

Our earlier studies determined that pS264-AQP2 is observed in both the apical plasma membrane and intracellular compartments associated with the early endocytic pathway after dDAVP treatment. To examine whether a similar mechanism existed for pS269-AQP2, Brattleboro rats were treated with a single intravenous injection of vehicle or dDAVP, and

after 15 or 60 min, kidneys were perfusion fixed. Double immunofluorescence labeling showed no colocalization of pS269-AQP2 with EEA1-positive compartments or Cathepsin-D-positive compartments at both time points examined (Figure 8). In contrast, total AQP2 was observed in association with clathrin-coated vesicles, early endocytic compartments, and lysosomal compartments after AVP stimulation (Figure 8). The localization of AQP2 to these compartments was confirmed by immunogold electron microscopy (Figure 9). Furthermore, immunogold electron microscopy using an antibody directed against the NH_2-terminus of AQP2 confirmed the localization of AQP2 in lysosomes (Figure S1).

Long-term AVP treatment resulted in increased pS269-AQP2 in the apical plasma membrane domain. To examine whether the increased pS269-AQP2 abundance observed after short-term dDAVP treatment was also present in response to long-term AVP stimulation, Brattleboro rats were administered either vehicle or dDAVP for 5 days by osmotic minipumps, and kidney sections were labeled with anti-pS269-AQP2. Confirming our earlier observation, pS269-AQP2 labeling is absent under control conditions (Figure 10a). Strong apical labeling is observed in response to continuous infusion of dDAVP (Figure 10b). Similarly, in Wistar rats water loaded for 5 days, pS269-AQP2 labeling is almost absent, whereas rats water-restricted for a similar time period showed strong apical labeling of pS269-AQP2 (Figure 10c–d).

DISCUSSION

In the mammalian kidney, AVP regulates the trafficking of AQP2-containing intracellular vesicles to the apical plasma membrane of the CD. This is a critical event for increasing the water permeability of the CD and producing concentrated urine. Phosphorylation of S256 in the COOH-terminal tail of AQP2 is essential for the membrane accumulation of AQP2.[2–4] In addition to S256, the COOH-terminal tail is phosphorylated at S261, S264, and S269. In our recent studies, we determined that two of the phosphorylated forms of AQP2, pS261-AQP2 and pS264-AQP2, are associated with different intracellular compartments,[5,8] although recent studies suggest that the phosphorylation status of AQP2 at S261 does not alter constitutive or regulated trafficking of AQP2.[10] In this study, we show that pS269-AQP2 is associated only with the apical plasma membrane domains of the CD, providing additional evidence that phosphorylated forms of AQP2 are localized to different cellular compartments, and further suggesting that dynamic poly-phosphorylation of AQP2 may be important for regulating AQP2 intracellular distribution.

A complete absence of labeling in CD-specific AQP2 knockout mice, as well as abolished labeling of kidney sections after pre-incubation of the antibody with a pS269 synthetic peptide, confirmed specificity of the antibody for pS269-AQP2. These data corroborate our previous observation regarding antibody specificity.[12]

A variety of immunolocalization techniques showed that pS269-AQP2 is associated only with apical plasma membrane domains throughout the CNT and CD. Unlike earlier observations of total AQP2,[13,14] we never observed the association of pS269-AQP2 with the basolateral membrane. These results are supported by *in vitro* cell culture studies. In MDCK cells stably transfected with a mutant AQP2 mimicking the charge state of pS269-AQP2 (S269D), AQP2 is localized to the plasma membrane under non-stimulated conditions.[12] Taken together, our data suggest that phosphorylation at S269 is involved with the apical targeting of AQP2.

In our earlier studies, we have shown that AVP can regulate acutely the degree of phosphorylation at each of the four serine residues at the COOH terminus tail of AQP2.[7,12] In this study, we find that acute dDAVP administration to rats *in vivo* recapitulates our

previous *in vitro* findings. After 30 min of dDAVP administration, pS269-AQP2 abundance increased in two different animal models. Immunohistochemistry determined that the increased pS269-AQP2 abundance occurred exclusively at the apical plasma membrane. Unlike pS256-AQP2, pS269-AQP2 was not observed in the absence of AVP, indicating that AVP is essential for phosphorylation at this site. Long-term AVP treatment resulted in a similar distribution of pS269-AQP2.

We have shown earlier that in the CD, there is time-dependent redistribution of pS264-AQP2 in response to dDAVP stimulation from predominantly intracellular vesicles to both the basolateral and apical plasma membranes.[8,9] In addition, a proportion of pS264-AQP2 can be observed in early endosomal and recycling compartments. A major finding in this study is that pS269-AQP2 is always associated with the apical plasma membrane. pS269-AQP2 is never observed in EEA1-positive vesicles, Rab11-positive recycling vesicles, or Cathepsin D-positive lysosomes. In addition, although a small proportion of pS269-AQP2 colocalizes with Adaptin-β positive compartments, we observed numerous distinct Adaptin-β positive, pS269-AQP2-negative compartments. This suggests that pS269-AQP2 could potentially 'escape' endocytosis and remain at the cell surface. These results for pS269-AQP2 may explain a earlier observation that a proportion of total AQP2 is located in 'endocytosis-resistant' membrane domains after AVP treatment.[15] Another explanation for our results is that the fraction of AQP2 that is endocytosed from the plasma membrane is immediately dephosphorylated at S269. Further studies utilizing cell models are required to elucidate these possibilities. In contrast to pS269-AQP2, using both confocal microscopy and immunogold electron microscopy, we detected total AQP2 in clathrin-coated vesicles, early endosomes, and lysosomes in CD principal cells after AVP treatment. Our finding that, using antibodies targeted against both the N and C termini, a proportion of total AQP2 localizes to lysosomes is novel and in contrast to earlier observations.[16] Our results provide evidence for a pathway of AQP2 degradation in CD principal cells.

The AVP-regulated accumulation of AQP2 at the apical plasma membrane is believed to be because of both an increased rate of exocytosis and decreased endocytosis.[17–19] In principle, phosphorylation of S269 could influence either process. From our results described here, and our previous observation that a mutant AQP2 mimicking the charge state of S269-AQP2 (S269D) is localized to the plasma membrane,[12] we propose that S269 phosphorylation is a mechanism that inhibits AQP2 endocytosis by allowing the protein to be sequestered in the plasma membrane or held out of clathrin-mediated endocytosis. Recent studies by Kamsteeg *et al.*[11] demonstrated conclusively that AQP2 is a short chain ubiquitinated at position K270 and that ubiquitination of AQP2 increases its rate of endocytosis. Theoretically, S269 phosphorylation may regulate the degree of ubiquitination and thus regulate its endocytosis. Future studies using cell-based models will be required to examine this hypothesis. Alternatively, as S269 is located in a putative type I PDZ ligand domain (SKA) at the C terminus of AQP2, S269 phosphorylation may alter the efficiency of binding of AQP2 to PDZ domain-containing proteins,[20,21] many of which are expressed in the IMCD.[22] The consensus class I PDZ ligand motif (-S/T-X-ϕ, where ϕ is any hydrophobic amino acid) is conserved in AQP2 from all mammalian sequences to date, with only a conserved S versus T variation at the −3 position relative to the COOH-terminus in humans. This high degree of conservation between species makes it highly likely that this motif plays some role in the interaction of AQP2 with other proteins at the plasma membrane. Future studies will be required to determine whether modification of this motif can influence the plasma membrane localization of AQP2.

MATERIALS AND METHODS

Materials

An affinity-purified rabbit polyclonal antibody (anti-pS269) was generated against a proprietary sequence from the COOH terminus of rat AQP2 that included pS269 (PhosphoSolutions, Aurora, CA, USA). Initial characterization of the anti-pS269 antibody determined that the antibody was specific for the pS269-AQP2 isoform.[12] In addition, a total AQP2 antibody against the N terminus (N-20, Santa Cruz, CA, USA) of rat AQP2, a total AQP2 antibody corresponding to amino acids in the COOH terminus upstream from the polyphosphorylated region of rat AQP2,[12] an affinity-purified antibody anti-pS256, which recognizes AQP2 phosphorylated at Ser-256,[23] and an affinity-purified antibody against β1-[H^+]ATPase[24] were used. Commercial antibodies used were mouse monoclonal antibodies against calbindin D-28K (Research Diagnostics, Concord, MA, USA), E-cadherin (BD Biosciences, Franklin Lakes, NJ, USA), early endosome-associated protein (EEA1), Golgi SNARE 28 (GS28), p115, Vti1a, Adaptin-β, (all from BD Transduction Laboratories, Franklin Lakes, NJ, USA), and a goat polyclonal antibody against Cathepsin D (Research Diagnostics).

Phosphatase treatment—Dephosphorylation of paraffin-embedded sections using calf intestinal alkaline phosphatase (Sigma, Brondby, Denmark) was performed as described earlier,[25] with minor modifications. After blocking of free aldehyde groups, sections were rinsed five times in alkaline phosphatase buffer (100 mM Tris, 50 μM $CaCl_2$, 0.1 mM $MgCl_2$, 8.4 μM leupeptin, 4 mM Pefablock, pH 9.0). Later, the sections were incubated in alkaline phosphatase buffer with or without calf intestinal alkaline phosphatase (~ 130 units/ml) in a water bath with constant agitation at 35 °C for 2.5 h.

Animal studies

All animal protocols were approved by the boards of the Institute of Anatomy and Institute of Clinical Medicine (University of Aarhus) in accordance to the licenses for the use of experimental animals issued by the Danish Ministry of Justice.

Protocol 1. *Normal Wistar rats, normal C57/BL6J mice, and CD-specific knockout mice.* CD-specific knockout mice and wild-type controls were obtained from an in-house stock.[26] Animals were maintained on standard rodent diet and had free access to water. Kidneys were perfusion fixed with 3% paraformaldehyde in 0.1 M sodium cacolydate, and pH 7.4 after anesthesia with isoflurane.

Protocol 2. *Short-term dDAVP infusion of Wistar rats.* Before the experiment, rats had free access to water and standard rat chow. Four rats were treated with subcutaneous injections of 1 ng dDAVP (Sigma-Aldrich, Brondby, Denmark) in 200 μl saline per animal, and four vehicle-injected rats served as controls. After 30 min, rats were anesthetized and kidneys were perfusion fixed. Between dDAVP injection and perfusion fixation rats had free access to water but not food.

Protocol 3. *Short-term dDAVP infusion of Brattleboro rats.* Homozygous Brattleboro rats deficient in AVP were maintained on standard rat chow with free access to water. Eight rats were treated with intravenous injection of 1 ng of dDAVP in 200 μl saline per animal, and eight saline-injected rats served as controls. The rats (four rats for each group) were anesthetized after 15 or 60 min and kidneys were perfusion fixed as described above. Between injection of dDAVP and fixation of the kidney, the 60-min group had free access to water but not food. The 15-min group was kept under anesthesia.

Protocol 4. *Long-term dDAVP infusion of Brattleboro rats.* Before experiments, rats had free access to standard rodent diet and water. Rats (six for each group) were implanted subcutaneously with osmotic minipumps (Alzet, Cupertino, CA, USA) delivering either 5 ng/h dDAVP or isotonic saline. After 5 days, the rats were anesthetized by halothane and kidneys were perfusion fixed.

Protocol 5. *Water loading/restriction of Wistar rats.* Rats were kept in metabolic cages and fed a gelled diet containing either 15 ml water (water restricted) or 45 ml water (water loaded) as described earlier.[27] After 5 days, rats were anesthetized and kidneys perfusion fixed.

Preparation of tissue for immunogold electron microscopy

Fixed tissue blocks from the kidney inner medulla were infiltrated with 2.3 M sucrose for 30 min and frozen in liquid nitrogen. Frozen tissue blocks were subjected to cryosubstitution and Lowicryl HM20 embedding. Lowicryl sections of 80 nm were cut on a Reichert Ultracut S and were pre-incubated with 0.05 M Tris, pH 7.4, 0.1% Triton X-100 (TBST) containing 0.1% sodium borohydride and 0.05 M glycine followed by incubation with TBST containing 0.2% skimmed milk. Pre-incubation was followed by incubation with anti-pS269 (1:250 dilution) and labeling was visualized with goat anti-rabbit IgG conjugated to 10-nm colloidal gold particles. Grids were stained with uranyl acetate for 10 min and with lead citrate for 5 s.

Semiquantitative immunoblotting

Preparation of protein samples, sodium dodecyl sulfate polyacrylamide gel electrophoresis and immunoblotting were performed as described earlier.[13] Antibodies used were affinity-purified anti-pS269 (1:250 dilution), anti-AQP2 (N-20, 1:2000 dilution), and β-actin (Sigma, 1:5000 dilution). Quantitative data are presented as mean ± s.e. Data were analyzed by one-way analysis of variance followed by Bonferroni's multiple-comparisons test. Multiple-comparisons tests were only applied when a significant difference was determined in the analysis of variance ($P < 0.05$). P-values < 0.05 were considered statistically significant.

Immunolabeling of kidney sections

This technique has been described in detail earlier.[13] Representative images from a minimum of four animals for each condition are shown. Light microscopy was carried out with a Leica DMRE microscope (Leica Microsystems, Herlev, Denmark).

Confocal laser scanning microscopy

Leica TCS SL (SP2) laser confocal microscope and Leica Confocal Software were used for imaging of the kidney tissue sections. Images were taken using an HCX PL APO ×63 oil objective lens.

Assessment of colocalization

To quantify the degree of colocalization, high-resolution images from different experimental rat kidney sections (at least eight images for each condition) were obtained sequentially using a 488-nm laser line and emission between 505 and 540 nm for Alexa 488, and a 546-nm laser line and emission between 570 and 620 nm for Alexa 546/555. Quantification of colocalization was performed using ImageJ software package (colocalization threshold analysis) and visual assessment of the staining pattern. Pearson's correlation coefficient (R) was used to determine the magnitude of correlation. A value of 1 represents perfect correlation; −1 represents perfect exclusion and zero represents random localization.

Supplementary Material

Refer to Web version on PubMed Central for supplementary material.

Acknowledgments

We thank Christian V. Westberg, Inger Merete Paulsen, Helle Høyer, Zhila Nikrozi, and Else-Merete Løcke for expert technical assistance. Robert A. Fenton is supported by a Marie Curie Intra-European Fellowship and the Danish National Research Foundation (Danmarks Grundforskningsfond). Hanne B. Moeller is supported by the Faculty of Health Sciences, University of Aarhus. Funding to M.A. Knepper was provided by the Intramural Budget of the National Heart, Lung, and Blood Institute (National Institutes of Health Project ZO1-HL001285). The Water and Salt Research Center at the University of Aarhus is established and supported by the Danish National Research Foundation (Danmarks Grundforskningsfond). Additional funding was provided by The Nordic Centre of Excellence Program (NCoE) in Molecular Medicine and by an EU Marie Curie Training Network Program.

REFERENCES

1. Nielsen S, Chou CL, Marples D, et al. Vasopressin increases water permeability of kidney collecting duct by inducing translocation of aquaporin-CD water channels to plasma membrane. Proc Natl Acad Sci USA. 1995; 92:1013–1017. [PubMed: 7532304]
2. Fushimi K, Sasaki S, Marumo F. Phosphorylation of serine 256 is required for cAMP-dependent regulatory exocytosis of the aquaporin-2 water channel. J Biol Chem. 1997; 272:14800–14804. [PubMed: 9169447]
3. Katsura T, Gustafson CE, Ausiello DA, et al. Protein kinase A phosphorylation is involved in regulated exocytosis of aquaporin-2 in transfected LLC-PK1 cells. Am J Physiol. 1997; 272:F817–F822. [PubMed: 9227644]
4. van Balkom BW, Savelkoul PJ, Markovich D, et al. The role of putative phosphorylation sites in the targeting and shuttling of the aquaporin-2 water channel. J Biol Chem. 2002; 277:41473–41479. [PubMed: 12194985]
5. McDill BW, Li SZ, Kovach PA, et al. Congenital progressive hydronephrosis (cph) is caused by an S256L mutation in aquaporin-2 that affects its phosphorylation and apical membrane accumulation. Proc Natl Acad Sci USA. 2006; 103:6952–6957. [PubMed: 16641094]
6. Shi PP, Cao XR, Qu J, et al. Nephrogenic diabetes insipidus in mice caused by deleting COOH-terminal tail of aquaporin-2. Am J Physiol Renal Physiol. 2007; 292:F1334–F1344. [PubMed: 17229678]
7. Hoffert JD, Pisitkun T, Wang G, et al. Quantitative phosphoproteomics of vasopressin-sensitive renal cells: regulation of aquaporin-2 phosphorylation at two sites. Proc Natl Acad Sci USA. 2006; 103:7159–7164. [PubMed: 16641100]
8. Fenton RA, Moeller HB, Hoffert JD, et al. Acute regulation of aquaporin-2 phosphorylation at Ser-264 by vasopressin. Proc Natl Acad Sci USA. 2008; 105:3134–3139. [PubMed: 18287043]
9. Hoffert JD, Nielsen J, Yu MJ, et al. Dynamics of aquaporin-2 serine-261 phosphorylation in response to short-term vasopressin treatment in collecting duct. Am J Physiol Renal Physiol. 2007; 292:F691–F700. [PubMed: 16985212]
10. Lu HA, Matsuzaki T, Bouley R, et al. The phosphorylation state of serine 256 is dominant over that of serine 261 in the regulation of AQP2 trafficking in renal epithelial cells. Am J Physiol Renal Physiol. 2008; 295:F290–F294. [PubMed: 18434387]
11. Kamsteeg EJ, Hendriks G, Boone M, et al. Short-chain ubiquitination mediates the regulated endocytosis of the aquaporin-2 water channel. Proc Natl Acad Sci USA. 2006; 103:18344–18349. [PubMed: 17101973]
12. Hoffert JD, Fenton RA, Moeller HB, et al. Vasopressin-stimulated increase in phosphorylation at Ser-269 potentiates plasma membrane retention of aquaporin-2. J Biol Chem. 2008; 283:24617–24627. [PubMed: 18606813]
13. Christensen BM, Wang W, Frokiaer J, et al. Axial heterogeneity in basolateral AQP2 localization in rat kidney: effect of vasopressin. Am J Physiol Renal Physiol. 2003; 284:F701–F717. [PubMed: 12453871]

14. de Seigneux S, Nielsen J, Olesen ET, et al. Long-term aldosterone treatment induces decreased apical but increased basolateral expression of AQP2 in CCD of rat kidney. Am J Physiol Renal Physiol. 2007; 293:F87–F99. [PubMed: 17376764]
15. Bouley R, Hawthorn G, Russo LM, et al. Aquaporin 2 (AQP2) and vasopressin type 2 receptor (V2R) endocytosis in kidney epithelial cells: AQP2 is located in 'endocytosis-resistant' membrane domains after vasopressin treatment. Biol Cell. 2006; 98:215–232. [PubMed: 16563128]
16. Tajika Y, Matsuzaki T, Suzuki T, et al. Immunohistochemical characterization of the intracellular pool of water channel aquaporin-2 in the rat kidney. Anat Sci Int. 2002; 77:189–195. [PubMed: 12422412]
17. Nielsen S, Knepper MA. Vasopressin activates collecting duct urea transporters and water channels by distinct physical processes. Am J Physiol. 1993; 265:F204–F213. [PubMed: 8396342]
18. Brown D. The ins and outs of aquaporin-2 trafficking. Am J Physiol Renal Physiol. 2003; 284:F893–F901. [PubMed: 12676734]
19. Knepper MA, Nielsen S. Kinetic model of water and urea permeability regulation by vasopressin in collecting duct. Am J Physiol. 1993; 265:F214–F224. [PubMed: 8396343]
20. Noda Y, Horikawa S, Katayama Y, et al. Identification of a multiprotein 'motor' complex binding to water channel aquaporin-2. Biochem Biophys Res Commun. 2005; 330:1041–1047. [PubMed: 15823548]
21. Noda Y, Horikawa S, Furukawa T, et al. Aquaporin-2 trafficking is regulated by PDZ-domain containing protein SPA-1. FEBS Lett. 2004; 568:139–145. [PubMed: 15196935]
22. Yu MJ, Pisitkun T, Wang G, et al. LC-MS/MS analysis of apical and basolateral plasma membranes of rat renal collecting duct cells. Mol Cell Proteomics. 2006; 5:2131–2145. [PubMed: 16899541]
23. Nishimoto G, Zelenina M, Li D, et al. Arginine vasopressin stimulates phosphorylation of aquaporin-2 in rat renal tissue. Am J Physiol. 1999; 276:F254–F259. [PubMed: 9950956]
24. Nelson RD, Guo XL, Masood K, et al. Selectively amplified expression of an isoform of the vacuolar H(+)-ATPase 56-kilodalton subunit in renal intercalated cells. Proc Natl Acad Sci USA. 1992; 89:3541–3545. [PubMed: 1373501]
25. Sternberger LA, Sternberger NH. Monoclonal antibodies distinguish phosphorylated and nonphosphorylated forms of neurofilaments *in situ*. Proc Natl Acad Sci USA. 1983; 80:6126–6130. [PubMed: 6577472]
26. Rojek A, Fuchtbauer EM, Kwon TH, et al. Severe urinary concentrating defect in renal collecting duct-selective AQP2 conditional-knockout mice. Proc Natl Acad Sci USA. 2006; 103:6037–6042. [PubMed: 16581908]
27. Kim GH, Ecelbarger CA, Mitchell C, et al. Vasopressin increases Na-K-2Cl cotransporter expression in thick ascending limb of Henle's loop. Am J Physiol. 1999; 276:F96–F103. [PubMed: 9887085]

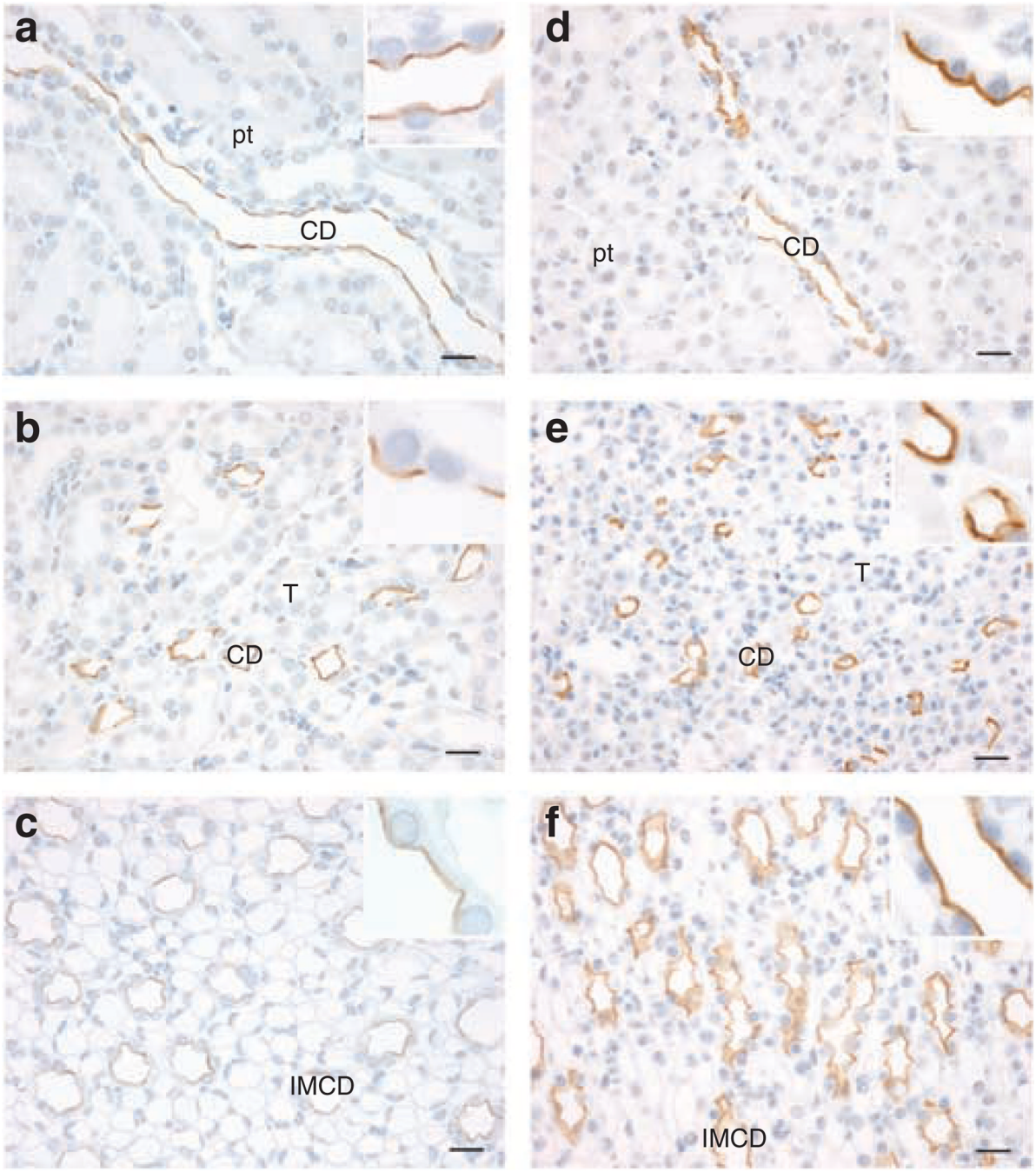

Figure 1. Immunoperoxidase labeling of pS269-AQP2 in the normal rat and mouse kidney

Labeling of pS269-AQP2 is observed throughout the collecting duct of normal rat kidney cortex (**a**), the inner stripe of outer medulla (**b**), and the inner medulla (**c**). A similar distribution is seen in the mouse kidney cortex (**d**), the inner stripe of outer medulla (**e**), and the inner medulla (**f**). Labeling is predominantly observed in the apical plasma membrane. Scale bar = 20 μm. CD, collecting duct; IMCD, inner medullary collecting duct; pt, proximal tubule; T, thick ascending limb.

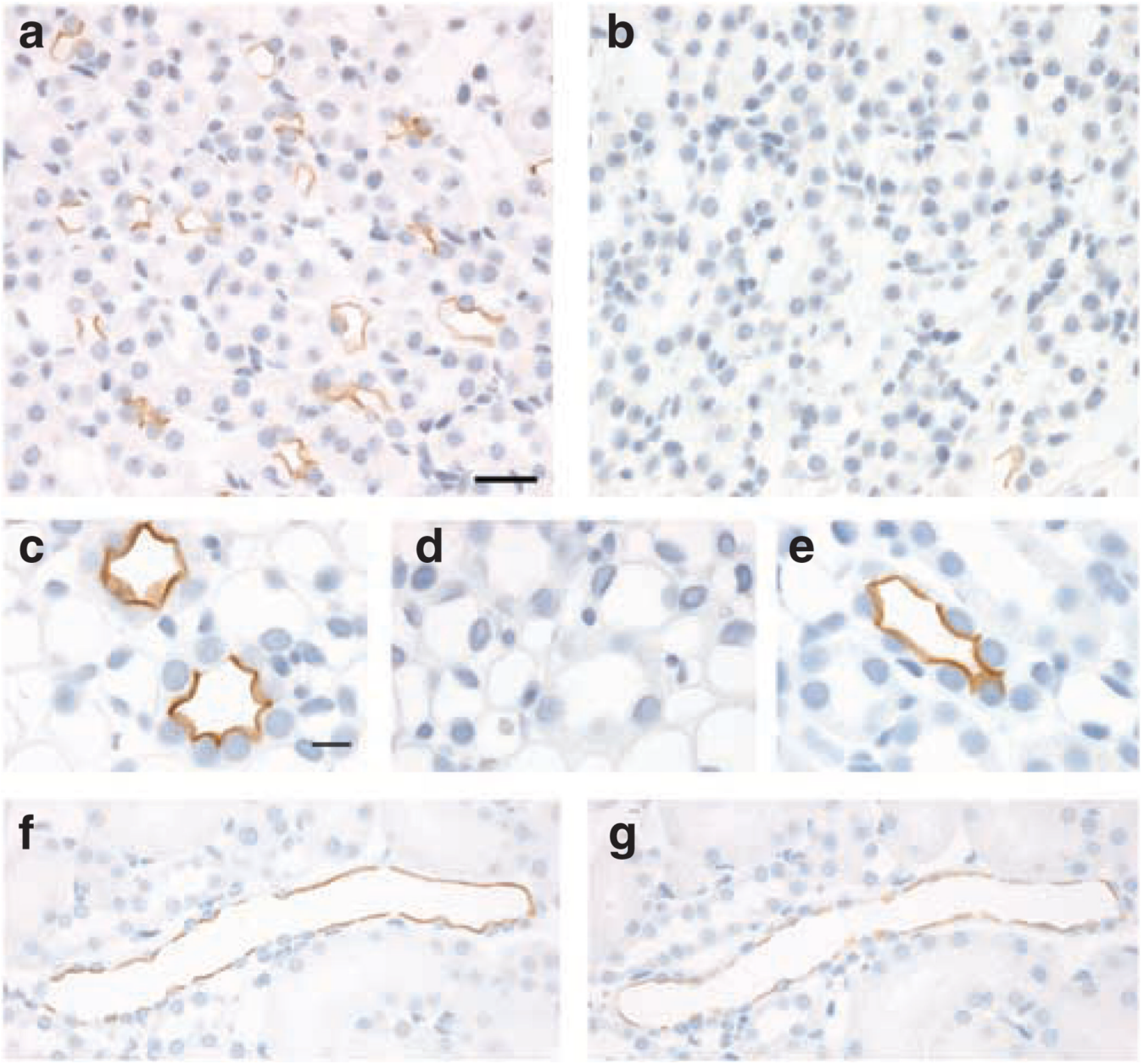

Figure 2. Specificity of pS269-AQP2 antibody

In AQP2 knockout mice, (**b**) there is a complete absence of immunoperoxidase labeling with the pS269-AQP2 antibody as compared with controls (**a**), indicating that the pS269-AQP2 antibody is specific for AQP2. Pre-absorption of anti-pS269 with pS269 peptide (**d**) resulted in the elimination of labeling in CD. In contrast, pre-incubation with either a non-phosphorylated peptide corresponding to the same region (**c**) or a peptide corresponding to pS264-AQP2 (**e**) did not affect labeling, indicating specificity of the antibody for pS269-AQP2. Labeling of pS269-AQP2 after phosphatase treatment of rat kidney serial sections (**g**) was dramatically reduced as compared with control (**f**). Scale bar = 20 μm.

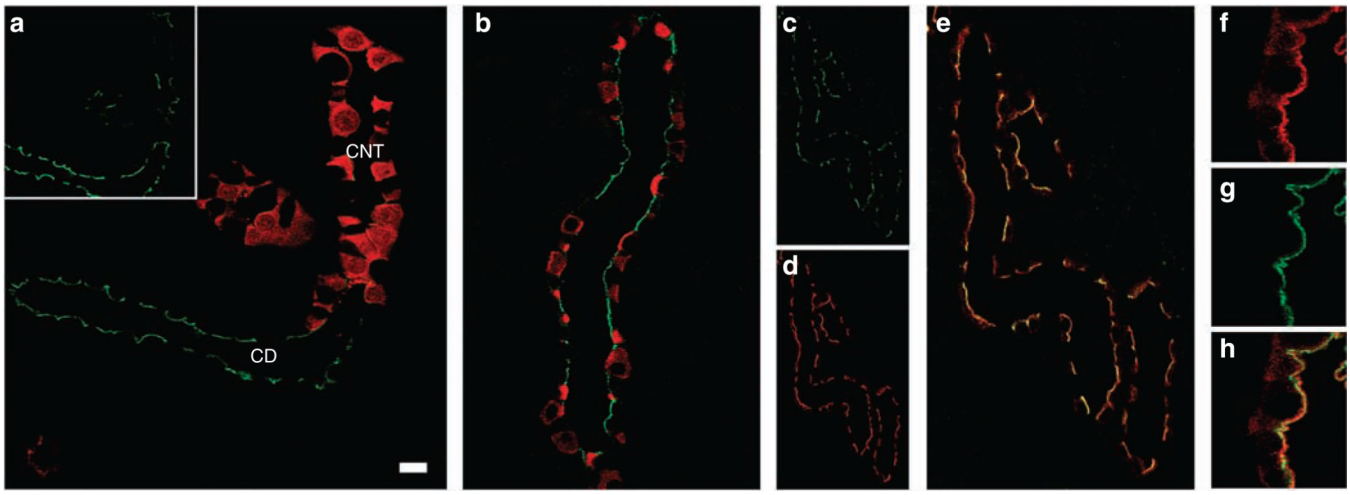

Figure 3. Confocal laser scanning microscopy of pS269-AQP2 in normal rat kidney

(**a**) Double immunofluorescence labeling of pS269-AQP2 (green, inset) and calbindin (red) identified that pS269-AQP2 is weakly expressed in connecting tubules. (**b**) Double immunofluorescence labeling of pS269-AQP2 (green) and [H^+]ATPase (red) determined that pS269-AQP2 is expressed in collecting duct principal cells. pS269-AQP2 (green, **c**) and total AQP2 (red, **d**) colocalize (yellow, **e**) at the apical plasma membrane of the collecting duct. At higher magnification, total AQP2 (**f**) is observed both on membranes and intracellularly. Colocalization with pS269-AQP2 (**g**) is restricted to the apical plasma membrane (**h**). CD, collecting duct; CNT, connecting tubule. Scale bar = 20 μm.

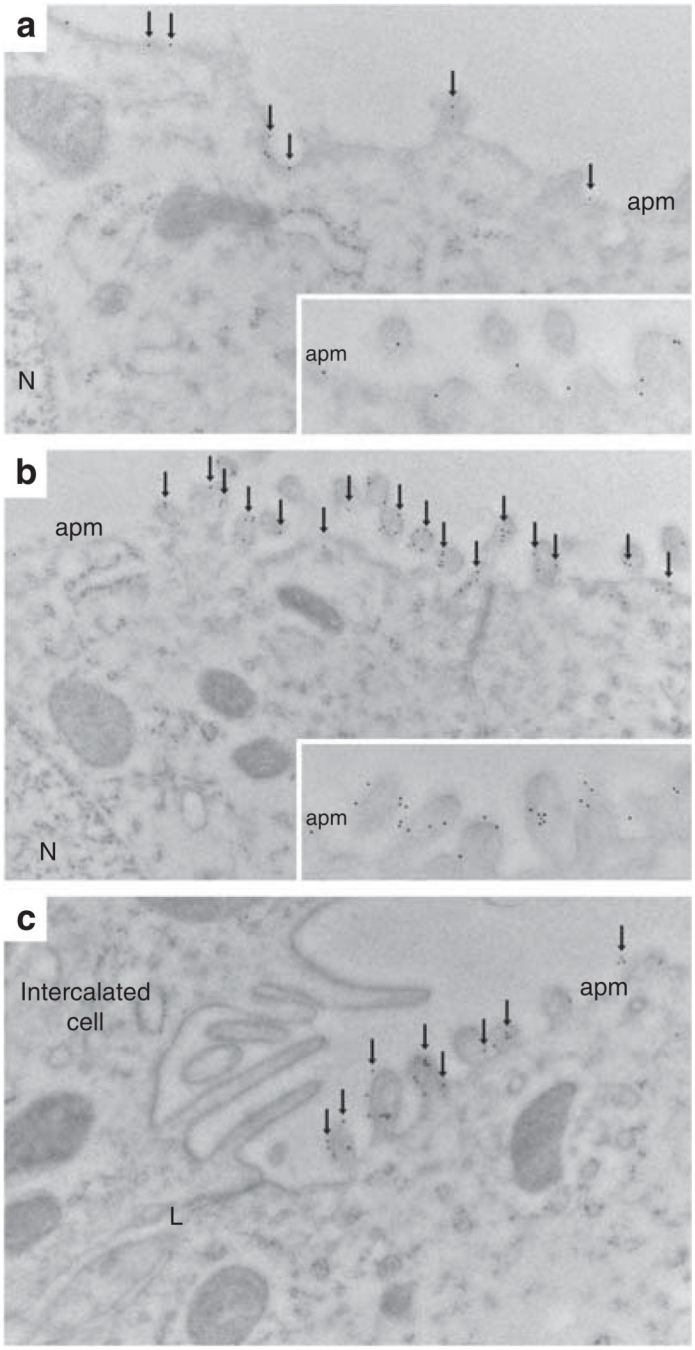

Figure 4. Immunoelectron microscopy of pS269-AQP2 in the normal rat kidney

(**a**) In normal Wistar rat kidney collecting duct principal cells, pS269-AQP2 (arrows) is observed in the apical plasma membrane domain (apm). At high magnification (inset), it is clear that all gold particles are associated with the membrane. (**b**) After dDAVP treatment (30 min), the number of gold particles increases in the apical plasma membrane domain (arrows), and at high magnification (inset), it is clear that all gold particles are associated with the membrane and no intracellular gold particles can be observed. (**c**) After dDAVP treatment, no gold particles are associated with the basolateral membrane. L, lateral membrane; N, nucleus.

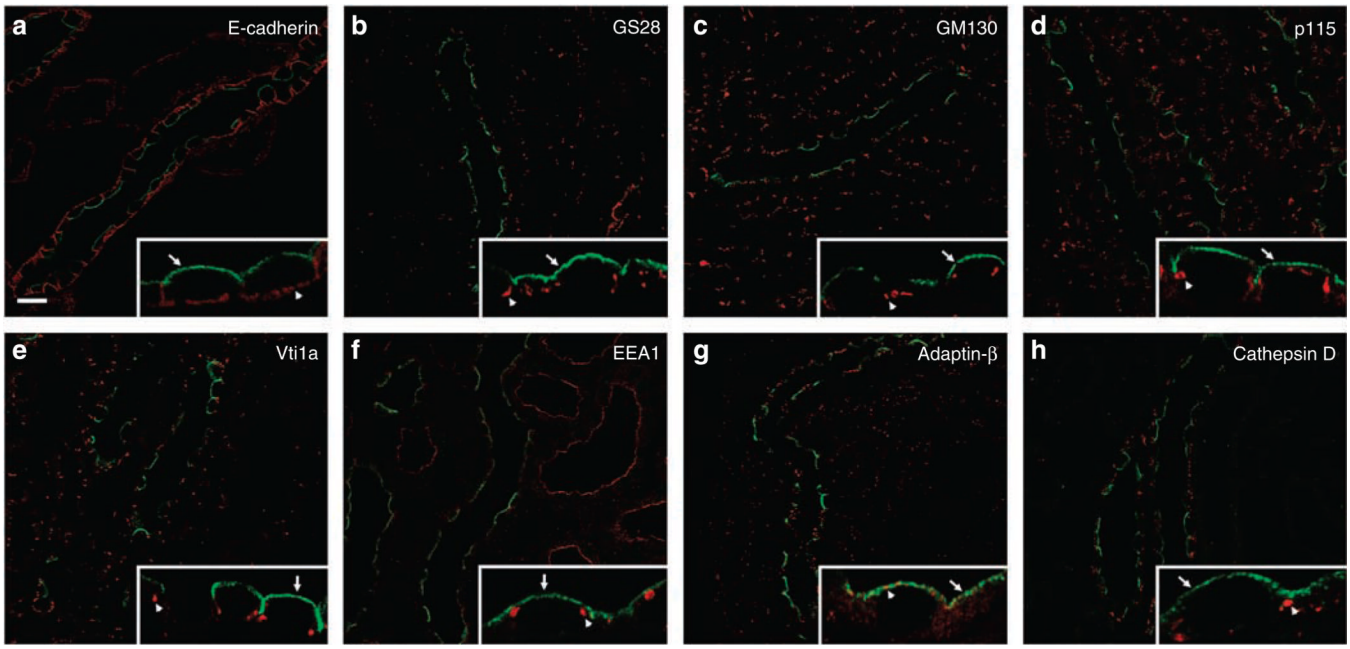

Figure 5. Subcellular distribution of pS269-AQP2 in normal rat kidney collecting duct

For all images, pS269-AQP2 is depicted in green, intracellular markers are depicted in red, and overlaid images show colocalized pixels in yellow. Insets in each panel represent high-magnification images of selected areas, with arrows indicating pS269-AQP2 and arrowheads for specific intracellular markers. No colocalization is observed with the basolateral membrane marker E-cadherin (**a**), the medial Golgi marker *GS28* (**b**), the *cis*-Golgi matrix marker GM130 (**c**), the *cis*-Golgi marker p115 (**d**), the *trans*-Golgi network marker *Vti1a* (**e**), the early endosome marker EEA1 (**f**), and the lysosomal marker Cathepsin D (**h**). A small degree of colocalization is observed with the clathrin-coated vesicle marker Adaptin-β at the apical plasma membrane, but distinct Adaptin-β-positive compartments are also observed (**g**). See Supplementary Table 1 for statistical comparison. Scale bar = 20 μm.

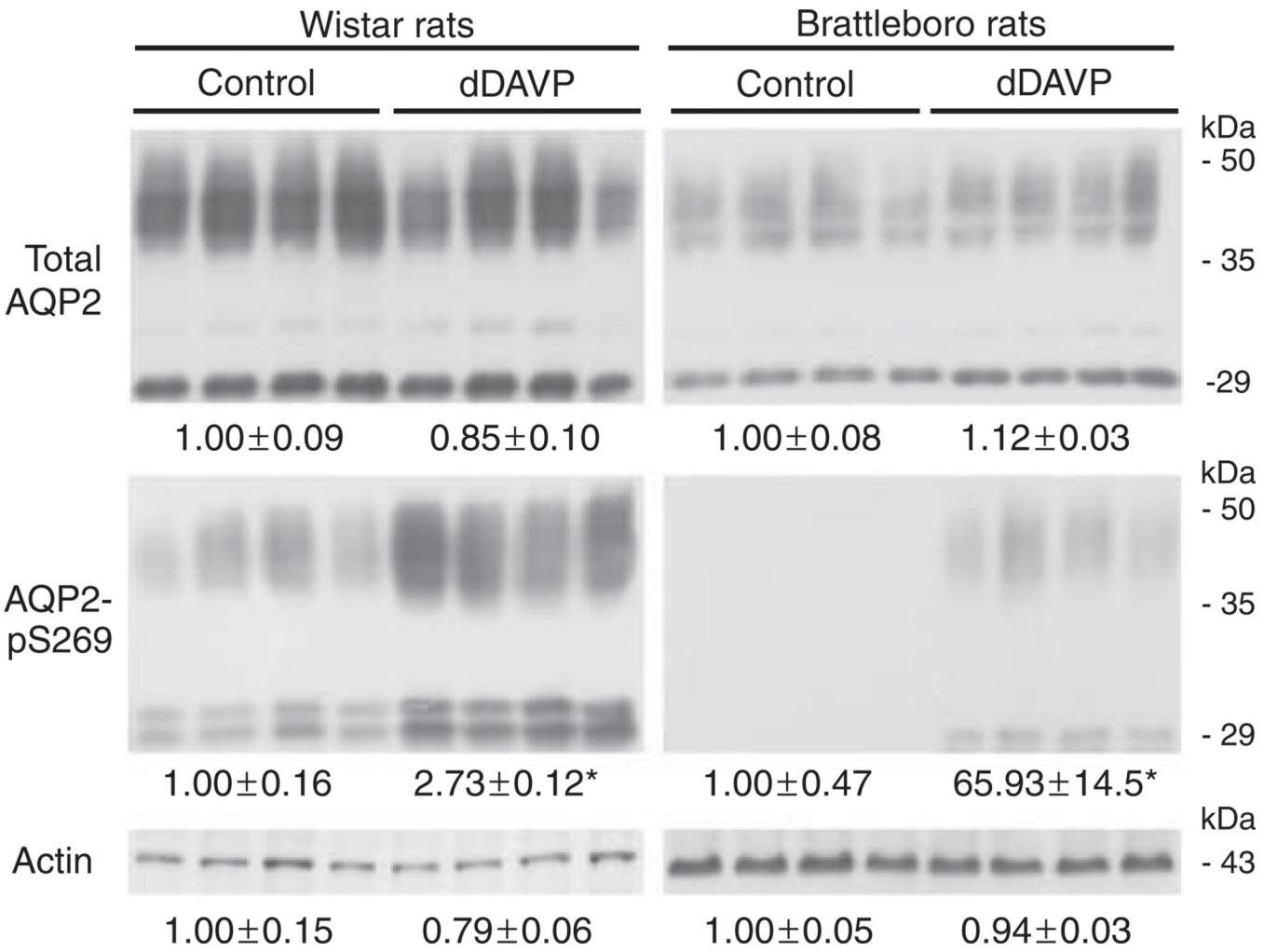

Figure 6. Short-term vasopressin treatment increases abundance of pS269-AQP2 *in vivo*

Immunoblots of inner medulla homogenates from Wistar rats and Brattleboro rats treated with dDAVP for 30 min. Each lane represents a sample from a different rat. Values are mean band densities (± s.e.) normalized such that the mean for the control rats is defined as 1. In Brattleboro rats, under control conditions pS269-AQP2 is not detectable, thus the mean band density value is arbitrary. Abundance of total AQP2 is not significantly changed after dDAVP treatment, whereas pS269-AQP2 abundance increases significantly. Immunoblotting using actin confirmed equal loading. *Significant change in mean band densities between groups.

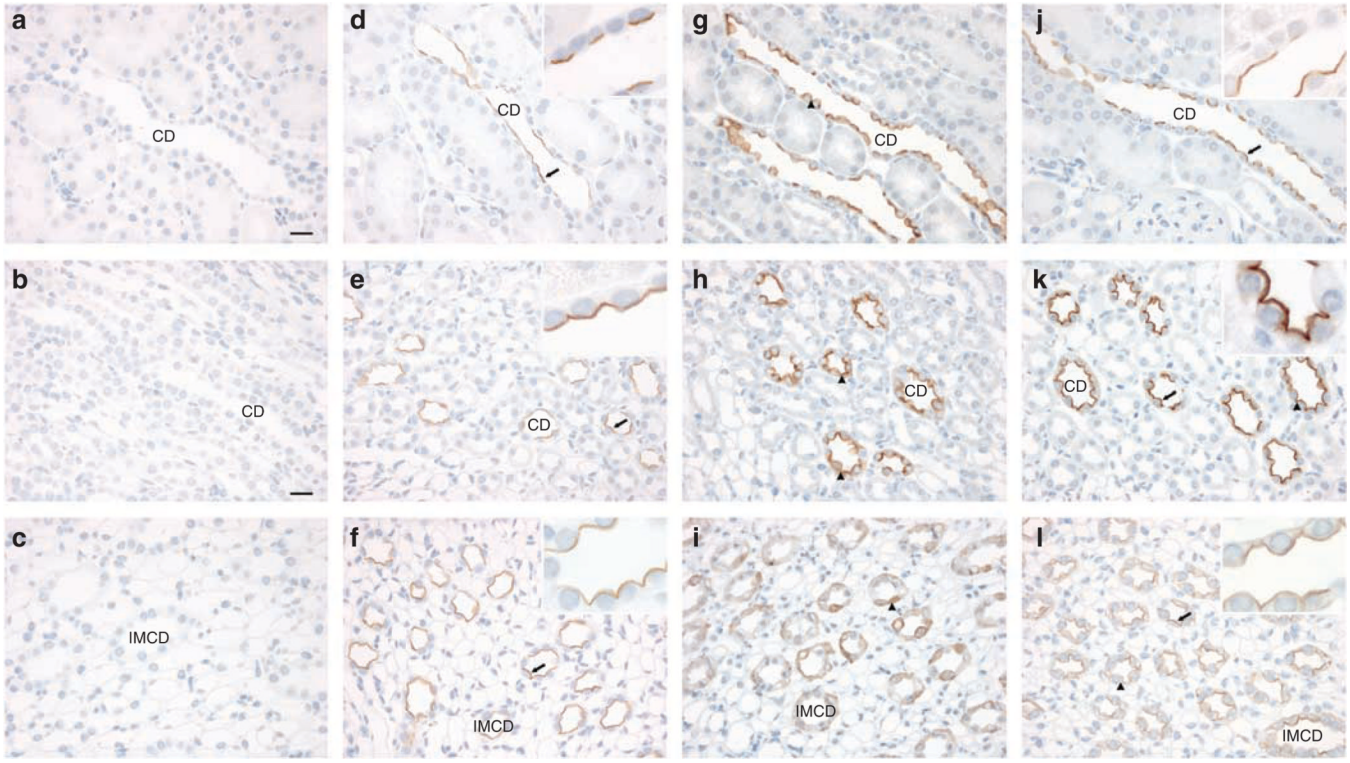

Figure 7. Short-term vasopressin exposure increases pS269-AQP2 abundance in the apical plasma membrane

Brattleboro rats were treated with either vehicle or dDAVP for 20 min and kidneys sections labeled with anti-pS269. Under control conditions, no labeling is apparent in the cortex (**a**), the inner stripe of outer medulla (**b**), and the inner medulla (**c**), whereas strong apical labeling (arrows) is observed in response to dDAVP (**d**–**f**, and insets). In contrast, pS256-AQP2 is observed in all regions under control conditions (**g**–**i**, arrowheads) and labeling intensity increases predominantly in the apical plasma membrane in response to dDAVP treatment (**j**–**l**, and insets). Scale bar = 20 μm. CD, collecting duct; IMCD, inner medullary collecting duct.

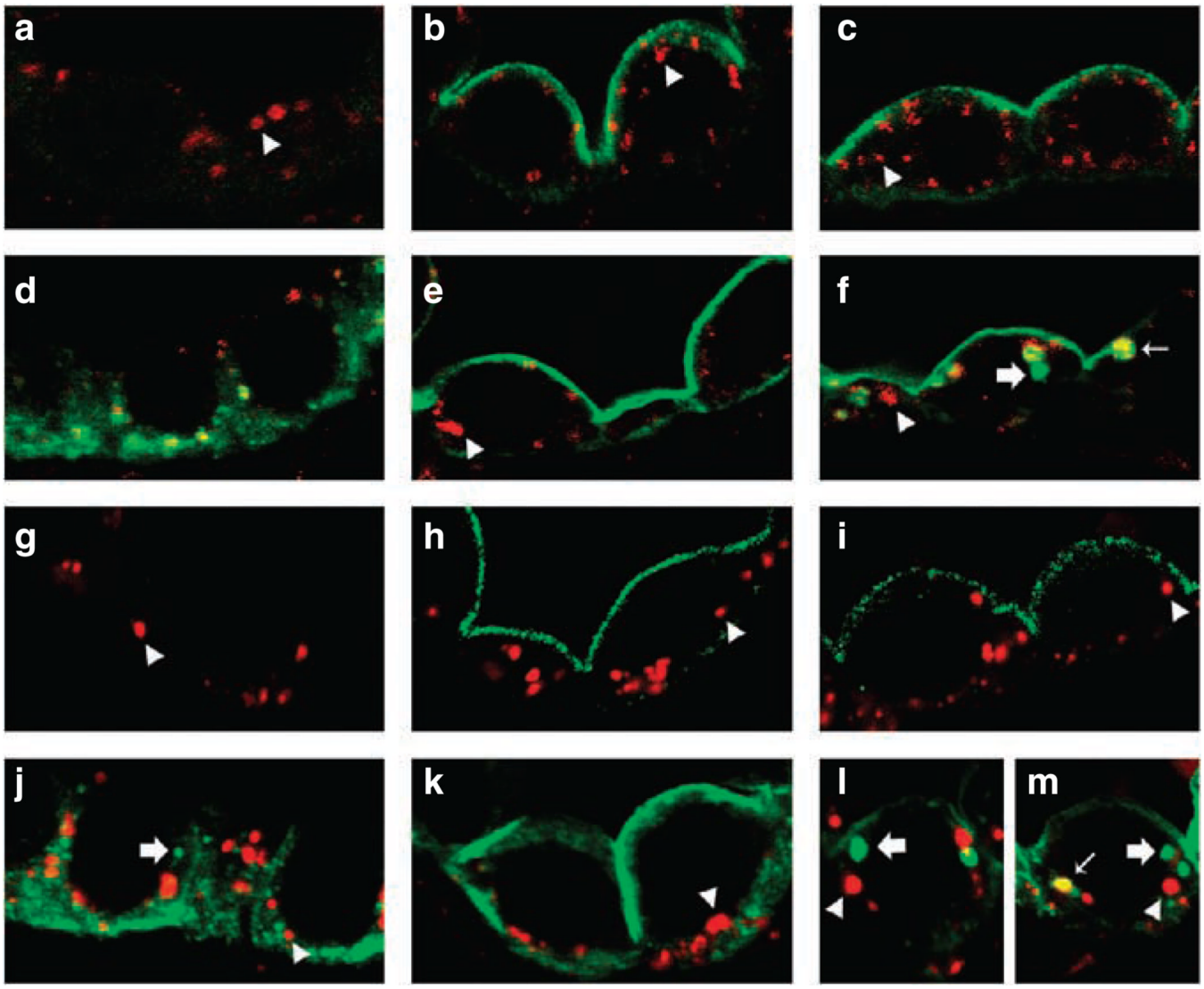

Figure 8. pS269-AQP2 is not associated with early endosomes or lysosomes after short-term dDAVP administration

Brattleboro rats were treated with either vehicle or dDAVP (15 and 60 min) and double immunofluorescence labeling was performed. Labeling of AQP2 is depicted in green and subcellular markers in red. Colocalization is indicated by a yellow pseudocolor and thin arrows. Arrowheads indicate distinct vesicles labeled with subcellular markers. Thick arrows indicate distinct AQP2-containing vesicles. pS269-AQP2 and EEA1-positive vesicles were not associated after vehicle, 15, or 60 min of dDAVP treatment (**a**, **b**, and **c**). In contrast, total AQP2 and EEA1-positive vesicles colocalized either under control conditions (**d**) or after 60 min of dDAVP treatment (**f**), but not after 15 min of dDAVP administration (**e**). Zero colocalization was observed between anti-pS269 and Cathepsin D at all time points (**g**, **h**, and **i**). Under control conditions or after 15 min dDAVP, no colocalization was observed between total AQP2 and Cathepsin D (**j**). After 60 min of treatment, although distinct AQP2-containing vesicles and Cathepsin D-positive vesicles were apparent (**l**), a proportion of AQP2 colocalized with Cathepsin D (**m**).

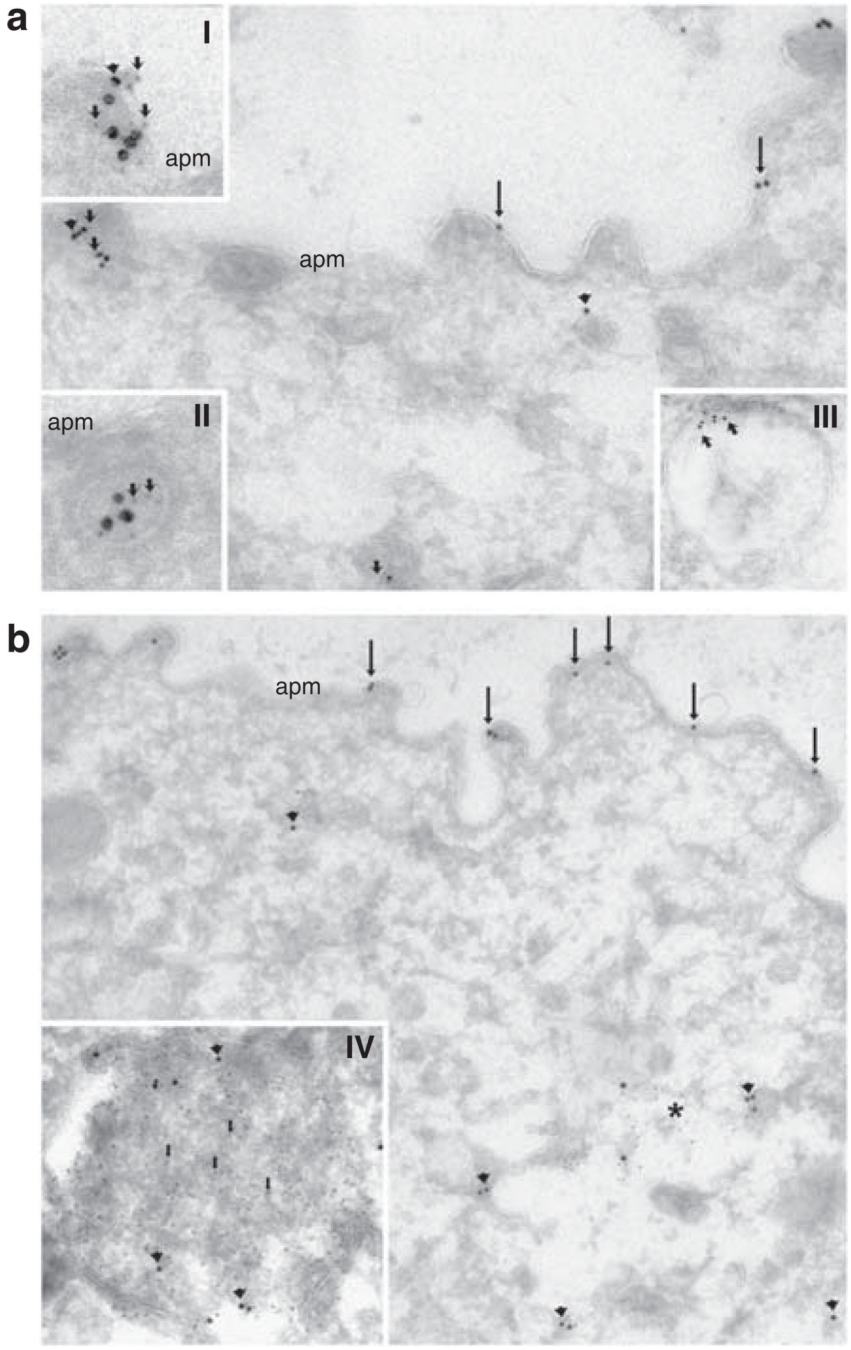

Figure 9. Total AQP2 is associated with clathrin-coated vesicles, early endosomes, and lysosomes

Brattleboro rats were treated with dDAVP for 60 min and immunogold electron microscopy was performed using an antibody targeted against the N terminus of rat AQP2. (**a**) In collecting duct principal cells, total AQP2 (large gold particles) is observed in the apical plasma membrane domain (arrows) and intracellularly (arrowheads). In some regions, AQP2 is associated with the clathrin-coated vesicle marker Adaptin-β (small gold particles, small arrows) at the apical plasma membrane (I) and in distinct subapical vesicles (II). Total AQP2 is also observed in early endosomes (III). (**b**) Total AQP2 (large gold particles) is associated with the apical plasma membrane domain (arrows) and distinct intracellular

vesicles (arrowheads). In addition, in some regions (*), total AQP2 colocalizes with the lysosomal marker cathepsin-D (small gold particles). At high magnification (IV), a single-distinct lysosomal structure can be observed containing cathepsin-D (small gold particles, arrows) and AQP2 (large gold particles, arrowheads). apm, apical plasma membrane.

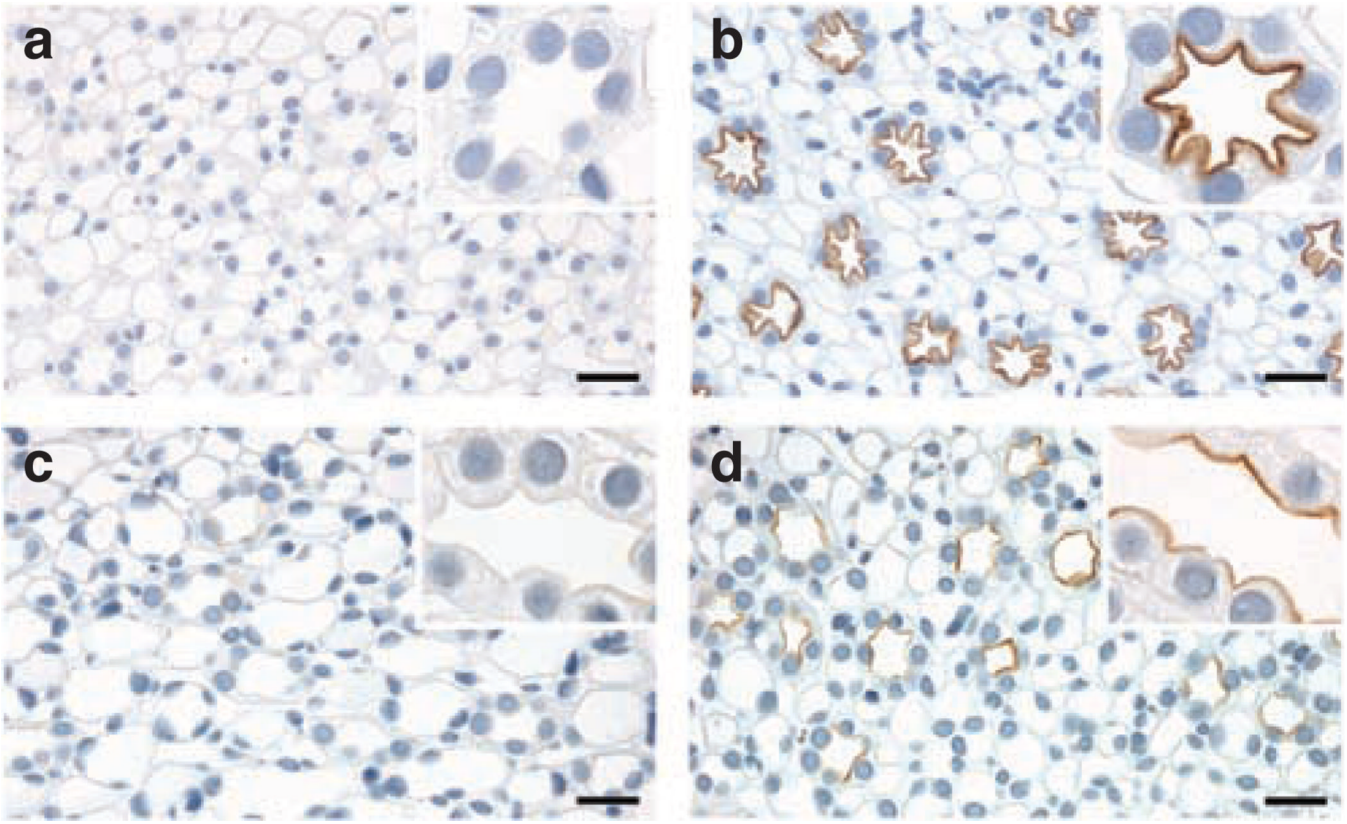

Figure 10. Long-term vasopressin exposure increases pS269-AQP2 abundance in the apical plasma membrane

Brattleboro rats were administered either vehicle or dDAVP for 5 days by osmotic minipumps. Under control conditions, pS269-AQP2 labeling is absent (**a**). Strong apical labeling is observed in response to dDAVP (**b**). Similarly, in Wistar rats water loaded for 5 days (**c**), pS269-AQP2 labeling was absent, whereas rats water restricted for a similar time period showed strong labeling of pS269-AQP2 only in the apical plasma membrane (**d**). Insets represent high magnification. Scale bar = 20 μm.